

Large particulate matter in the Western Mediterranean

I. LPM distribution related to mesoscale hydrodynamics

G. Gorsky^{a,*}, L. Prieur^a, I. Taupier-Letage^b, L. Stemmann^{a,1}, M. Picheral^a

^aLaboratoire d'Océanographie de Villefranche sur mer (LOV), UPMC/CNRS/SDU, France

^bLaboratoire d'Océanographie et Biogéochimie (LOB), CNRS/COM/Université de la Méditerranée, France

Received 24 November 2000; accepted 3 December 2001

Abstract

The relationship between mesoscale hydrodynamics and the distribution of large particulate matter (LPM, particles larger than 200 μm) in the first 1000 m of the Western Mediterranean basin was studied with a microprocessor-driven CTD-video package, the Underwater Video Profiler (UVP). Observations made during the last decade showed that, in late spring and summer, LPM concentration was high in the coastal part of the Western Mediterranean basin at the shelf break and near the continental slope (computed maximum: 149 $\mu\text{g C l}^{-1}$ between 0 and 100 m near the Spanish coast of the Gibraltar Strait). LPM concentration decreased further offshore into the central Mediterranean Sea where, below 100 m, it remained uniformly low, ranging from 2 to 4 $\mu\text{g C l}^{-1}$. However, a strong variability was observed in the different mesoscale structures such as the Almeria–Oran jet in the Alboran Sea or the Algerian eddies. LPM concentration was up to one order of magnitude higher in fronts and eddies than in the adjacent oligotrophic Mediterranean waters (i.e. 35 vs. 8 $\mu\text{g C l}^{-1}$ in the Alboran Sea or 16 vs. 3 $\mu\text{g C l}^{-1}$ in a small shear cyclonic eddy). Our observations suggest that LPM spatial heterogeneity generated by the upper layer mesoscale hydrodynamics extends into deeper layers. Consequently, the superficial mesoscale dynamics may significantly contribute to the biogeochemical cycling between the upper and meso-pelagic layers. © 2002 Elsevier Science B.V. All rights reserved.

Keywords: Large particulate matter; Western Mediterranean; Mesoscale hydrodynamics

1. Introduction

Vertical export of atmospheric CO_2 as detritus is a complex process beginning with primary production

in the epipelagic zone of the ocean. Atmosphere/sea interactions determine the nature and extent of superficial circulation patterns that in turn generate various mesoscale structures that can regulate the rate and intensity of the biological activity. For example, physical forcing influences the availability of nutrients, which might determine the level of primary and secondary production and by consequence the processes of remineralization and the vertical export of particulate matter.

* Corresponding author. Tel.: +33-4-93-76-3816; fax: +33-4-93-76-3834.

E-mail address: gorsky@obs-vlfr.fr (G. Gorsky).

¹ Present address: Department of Oceanography, Texas A&M University, College Station, TX-77843-3146, USA.

According to Bethoux et al. (1999), the Mediterranean is a miniature ocean where the effects of climatic and environmental variables on bio-physical coupling are easier to study than on oceanic scales. Several physical and ecosystem models have been developed to examine biological patchiness induced by energetic flow fields, such as the frontal regions of interacting gyres, eddies, jets or filaments. Mesoscale vertical motion can considerably influence the phytoplankton-nutrients system and can control the size structure of the phytoplankton and by consequence, the production and advection of the organic matter (Franks and Walstad, 1997; Rodriguez et al., 2001; Spall and Richards, 2000; Zakardjian and Prieur, 1998).

The ubiquity of the non-motile particles in the water column, large enough to be visible to the naked eye, has been known since the first scientific bathyscaphic dives (Suzuki and Kato, 1953). They named these particles as “marine snow”. Since then, marine snow aggregates have been observed everywhere in the world’s oceans and are recognized as the major conveyors of the superficial biomass to deep layers (Alldredge and Silver, 1988; Alldredge and McGuillivary, 1991; Gardner and Walsh, 1990; Graham et al., 2000; Honjo et al., 1984; Lampitt et al., 1993; MacIntyre et al., 1995; Stemmann et al., 2000). According to Jackson et al. (1995, 1997) and Syvitski et al. (1995), particles from 0.1 to 3 mm diameter account for most of the particulate matter mass suspended in oceanic and coastal waters and also for the major part of particles settling to the seafloor. Nevertheless, information on the spatial distribution and temporal dynamics of this large particulate matter and observations on the role of mesoscale structures on the processes of aggregation and vertical transport are rare.

In this paper, we describe the spatial distribution of large ($>200\ \mu\text{m}$) particulate matter (LPM) in different hydrological features. The detailed description of mesoscale structures was published elsewhere (see literature in corresponding chapters). Only data collected during the well-stratified period (June–September) within the last decade is presented in this paper. This data was collected using a new instrument, called the Underwater Video Profiler and was employed in different oceanographic programs in the Mediterranean. Here we discuss results concerning the Western Mediterranean basin.

2. General hydrological features in the Western Mediterranean Sea

2.1. Water characteristics

The Mediterranean Sea is a semi-enclosed sea that communicates with the Atlantic ocean through the narrow Strait of Gibraltar. Low salinity Atlantic water enters in the upper layer of the Gibraltar Strait and meet the Mediterranean water masses in the Alboran Sea creating highly energetic mesoscale structures such as jets, fronts, eddies, gyres. These structures are the sites of intense three-dimensional circulation, which is of great importance for the physical–biological coupling. Characteristics of Atlantic water are progressively modified through mixing and evaporation. In the Eastern Mediterranean air–sea interactions and oceanic conditions generate a downward mixing of surface waters, which forms the higher salinity and higher temperature Levantine Intermediate Water (LIW). This water flows into the western basin through the Strait of Sicily and along the northern coast. LIW can be entrained into the Algerian eddies from the Sardinian coast. The Winter Intermediate Water (WIW) is a sub-superficial product of winter surface cooling in the western basin, mainly in the Gulf of Lions. Here, the Western Mediterranean Deep Water (WMDW) is formed as a consequence of the strong heat loss due to the wind regime and to the subsequent deep convection. This process is enhanced by the cyclonic circulation in the northern part of the western basin. In the Tyrrhenian basin, the Tyrrhenian Deep Water (TDW) generates from the mixing of inflowing WMDW and LIW. The TDW by increasing the intensity of the deep circulation seems to play an important role in the western basin (Send et al., 1999).

2.2. Circulation patterns

Atlantic water with low nutrient concentration flows into the Mediterranean through the Strait of Gibraltar. Beneath this inflow, nutrient rich Mediterranean waters flow in the opposite direction. Because of the shallow sill, intensive mixing processes take place between the overlaying water masses. In addition, nutrient-rich North Atlantic Central Water is periodically injected to the Mediterranean and enriches the inflowing waters (Gomez et al., 2000).

These mixing processes stimulate high photosynthetic activity near the Spanish coast. In the Alboran Sea, the Atlantic inflow generates most often two anticyclonic gyres and proceeds toward the South as a jet (the Almeria–Oran jet). Near the Algerian coast, it becomes the Algerian Current, and flows eastward (~ 50 cm/s). This current is unstable and generates mesoscale anticyclonic eddies, ~ 50 – 100 km in diameter (Millot, 1985), which propagate eastward at a few km/day. The Algerian eddies can leave the Algerian slope (most often as they guided toward the North by the bathymetry in the Channel of Sardinia) and become open sea eddies. Eventually, they can move back close to the Algerian slope and interact with the meandering Algerian Current.

Near surface-circulation of the northwestern Mediterranean is linked to thermohaline processes and is driven by the atmospheric seasonality. The Northern Current (*sensu* Millot, 1999) originates in the Ligurian Sea and streams westward towards the Channel of Ibiza. Generally, in winter the current is narrow and flows near the coast, while in summer it is broad and shallow.

The Western Mediterranean is characterized by large mesoscale structures that generate intense density gradients. Eddies, filaments or jets are formed by the influx of Atlantic waters from the Alboran Sea (Arnone and La Violette, 1986; Lohrenz et al., 1988; Tintoré et al., 1998, 1991; Viudez et al., 1996). Anticyclonic and cyclonic eddies are created by the meandering Algerian Current (Arnone et al., 1990; Millot et al., 1997; Puillat et al., 2002; Taupier-Letage et al., *in press*). Convergence–divergence zones are generated by the Northern Current in the Ligurian Sea (Boucher et al., 1987; Millot, 1999; Send et al., 1999; Sournia et al., 1990).

2.3. Nutrients and carbon

The inflowing Atlantic waters are nutrient-depleted, while the Mediterranean outflow is nutrient-rich. Only 25% of the outflowing nutrient loss is compensated by the inflowing waters (Gomez et al., 2000). The main source of nutrients in the Mediterranean is of continental origin. Another mechanism for nutrient enrichment of the superficial layers is the deep vertical convection and the consequent mixing process that takes place during the WMDW

formation. New production is higher in the western basin than in the eastern Mediterranean, reaching between 13 and 24 g C m⁻² year⁻¹ (Bethoux et al., 1998). An additional part of the carbon export to deeper layers is the direct atmospheric input during the WIW and WMDW water formation. A wide range of nitrogen species of anthropogenic or natural origin is deposited in the Mediterranean through atmospheric input (Guerzoni et al., 1999). These can potentially account for 6–60% of the new production on an annual scale in coastal productive and oligotrophic zones, respectively. Therefore, the Mediterranean can be considered as a sink of CO₂ (Copin-Montegut, 1993). In the deep waters, the nitrate vs. phosphate ratio is unusually high (about 22, McGill, 1970; approximately 22 below 1000 m in the western basin, Moutin and Raimbault, 2002). The N/P ratio of atmospheric input is also high (~ 70 , Herut and Krom, 1996). Therefore, the ecosystem dynamics may be influenced by the probable phosphorus limitation.

2.4. Pelagic–benthic coupling

Danovaro et al. (1999) described seasonal changes in mass fluxes in the Mediterranean. According to these authors, the organic carbon flux is significantly correlated to the mass flux. The POC fluxes can be of one to two orders of magnitude higher in the western than in the eastern basin. While about 10% of the primary production can reach the sea floor in the Western Mediterranean, only about 1% will be available for the benthic fauna in the eastern part. These fauna react to the seasonal variation in the western but not in the eastern basin.

Along the water column and in the sediment, the particulate organic matter (POM) had similar gross composition and the sedimentary organic matter composition reflected the suspended POM composition (Danovaro et al., 1999). In oligotrophic midwater, the solubilisation of aggregates by attached bacteria may explain the low particle flux reaching the sea floor (Turley and Stutt, 2000). Near the Spanish Mediterranean continental slope, Puig et al. (2000) observed that the suspended particulate matter advective transport dominated over the vertical fluxes. Much more particulate matter carbon was carried along the slope in deep layers than found in the adjacent sediment

traps. The mid- and deep-water nepheloid layers may sequester high concentrations of POM.

3. Datasets

The vertical distribution of aggregates in different mesoscale structures has been determined since 1991 during several multidisciplinary oceanographic programs in the Western Mediterranean (Fig. 1). The data collected by the UVP can be consulted in the databanks given below.

(1) The eastern part of the Gibraltar Strait was studied during the European CANIGO project (Canary Islands Azores Gibraltar Observations). Eight stations were sampled in Strait of Gibraltar on board of R/V Cornide de Saavedra during September 1997 (Echevarria et al., in press). Here, we present data from three stations located in the Mediterranean side of the Strait ($35^{\circ}53'–36^{\circ}05' N$ and $5^{\circ}18'–5^{\circ}55' W$, ISMARE databank, see also the special issue on The Mediterranean Sea-Circulation, Strait Exchange and Dense

Water Formation, in Journal of Marine Systems, vol. 20, 1–442, 1999).

(2) The Almeria–Oran jet in the Alboran Sea was studied in June 1991 (from $35^{\circ}40'–37^{\circ}30' N$ and $0^{\circ}58'–2^{\circ}53' W$) during the French FRONTAL program (JGOFS/France databank, see also the special issue on Processes and Fluxes in the Geostrophic Almeria–Oran Front in Journal of Marine Systems, vol. 5, 187–399, 1994).

(3) The Algerian basin was investigated during the ELISA 1 cruise (Eddies and Leddies Interdisciplinary Study off Algeria) in summer 1997, as a part of the MATER (Mass Transfer and Ecosystem Response) European program ($37^{\circ}0'–38^{\circ}20' N$ and $3^{\circ}57'–7^{\circ}18' E$, <http://www.com.univ-mrs.fr/ELISA/>, SIS-MER databank, Taupier-Letage et al., in press).

(4) The Ligurian part of the Northern Current was examined in July 1995, during the MBP-Front (MesoBathyPelagic-Front), French FRONTAL program ($43^{\circ}25'–43^{\circ}40' N$ and $7^{\circ}21'–7^{\circ}52' E$). Results of this 4-year program were presented in Stemmann,

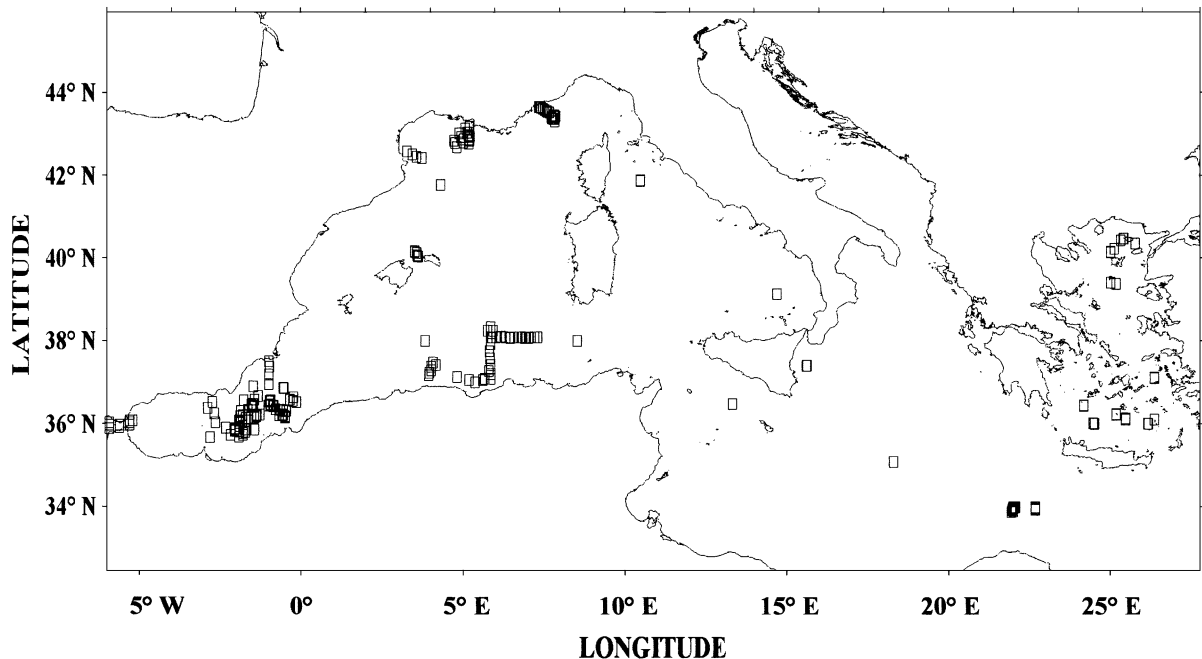


Fig. 1. The Western Mediterranean and the Aegean Sea (from JEBCO 97 Digital Atlas). Rectangles indicate the stations sampled by the Underwater Video Profiler during the last decade. Here, we describe only the western basin and specifically the large particulate matter (LPM) distribution in the Mediterranean part of the Gibraltar Straits, in the eastern Alboran Sea, in the Algerian basin, in the Ligurian Sea, in the Gulf of Lions and in the vicinity of the Balearic islands. Only two stations were sampled in the Thyrrenian Sea.

1998 and the data are in the JGOFS/France databank).

(5) The eastern part of Gulf of Lions was studied in July 1995, during the European EMPS (European Microbiology of Particulate Systems) MTP-I program (42°46′–43°10′ N and 5°12′–5°13′ E, EMPS EC databank).

(6) The western part of Gulf of Lions and Balearic Islands were examined in July 1995 during the European EUROMARGE MTP-I program (40°02′–42°34′ N and 3°17′–4°20′ E, JGOFS/France databank).

(7) The Alboran Sea, Algerian basin, Thyrrenian Sea and Ligurian Sea were studied in September 1999 during the PROSOPE cruise (Productivity of Pelagic Oceanic Systems), a JGOFS/France program. The coordinates of the stations are: 38°05′ N–5°12′ W, 38°25′ N–0°51′ W, 38°N–3°50′ E, 38°N–8°32′ E, 39°07′ N–14°42′ E, 41°52′ N–10°29′ E and 43°27′ N–7°50′ E, PROSOPE/JGOFS databank).

4. Methods

4.1. The Underwater Video Profiler (UVP)

The UVP (Gorsky et al., 1992, 2000) constructed at the Observatoire Océanologique in Villefranche sur mer, France (<http://www.obs-vlfr.fr/~pvm>) is a microprocessor driven instrument package. Model 3 consists of two video cameras and recorders for simultaneous image acquisition of undisturbed particles in a collimated slab of light delivered by two Chatwick-Helmut 54 W stroboscopes laterally illuminating the particles at a frequency of 25 Hz. A seabird 19 CTD, a fluorometer and a nephelometer (both from Chelsea Instruments) are mounted on the UVP steel frame. The UVP is lowered at a speed of 1 m s⁻¹ and data acquisition is performed during the descent. The volumes recorded by the two cameras are 1.3 and 6.5 l per image. Immediately after the vertical profile, the recorded sequence is digitized without compression and analyzed using two custom-made software programs and merged with the biophysical data. Each recorded object is detected (due to its light scatter on the dark background) and its different physical attributes are

measured and stored. Only particles comprising a given number of pixels, according to the calibrations, are taken into account. Laboratory calibrations were made for the different UVP models on a variety of natural particles. We calculated the regression between the particle apparent size and its real size measured by a stereomicroscope. All the particles >200 µm injected into the light slab were detected by the different UVPs. They were used for the conversion of particle surface and length to metric units following the equation $Sm = aSp^b$, where Sm is the area in mm² and Sp is the number of activated pixels for each particle after the A/D conversion. Equivalent spherical diameter (ESD) is calculated from the particle surface data following the equation $ESD = 2\sqrt{Sm/\pi}$. This value is used to estimate the marine snow dry (DW) and carbon weight ($DW = 8.8ESD^{1.125}$, from Alldredge and Gotschalk, 1988). Alldredge and Gotschalk (1988) and Alldredge (1998) photographed and collected hundreds of aggregates of different origin and showed that their mass content is a function of the equivalent spherical diameter regardless of their origin. These large aggregates were hand collected in the superficial waters and may differ in content from smaller deep-water particles. According to Alldredge (1998), the C and N content of marine snow can be estimated from the abundance and size profiles acquired by different in situ photo and video systems. We estimated the carbon content as 20% of the dry weight (proportion obtained for gelatinous matter; Alldredge, 1979; Chester and Stoner, 1974) calculated from the equation of Alldredge and Gotschalk (1988). Algae flocks and zooplankton were considered as LPM. Zooplankton density was from one to two orders of magnitude lower than the concentration of aggregates (Stemmann et al., 2000). This paper focuses on the LPM spatial distribution in the water column in relation with the upper layer mesoscale hydrodynamics. The carbon estimates are extrapolated from the particles surface measurements, therefore their value is only indicative. However, the linear relationship between their number and calculated mass (Stemmann, 1998) may render the use of carbon units acceptable. In the framework of JGOFS, the extrapolation to carbon mass may be of more use than using units such as number per volume. These estimations will be

refined by improved calibrations and in situ sampling of suspended particles using ROVs.

4.2. In-situ optical assessment of fine particulate matter

Water turbidity (caused by small particles) measured by light scattering nephelometers is expressed in formazin turbidity units (FTU). The comparison between a transmissometer and a nephelometer showed that the former was more sensitive to fresh coarse (up to tens of microns) superficial particulate matter, while the second to the finer, deeper, possibly resuspended matter (less than 10 μm in size) (Hall et al., 2000).

Only few turbidity (FTU) vs. suspended matter (mg l^{-1}) calibration data are found in the literature (Southerland et al., 2000). Guilén et al. (2000) calibrated backscattering nephelometers turbidity measurements against filtered suspended matter in the Western Mediterranean. Significant correlation coefficients of light scatter and particulate matter concentration were obtained for homogeneous population of particles.

Generally, the commercially available optical sensors (nephelometers or transmissometers) or filtration methods are used for the estimation of the organic matter vertical distribution. These methods estimate only the fraction of fine particles distribution. Here, we compare the fine particles distribution (in FTU units) to the distribution and fate of larger particles ($>200 \mu\text{m}$ ESD). For vertical profiles, where we have no optical sensors data, we grouped the UVP data into two size classes: 200–500 and $>500 \mu\text{m}$ ESD. Methods used for the UVP data treatment are described in Stemmann et al. (2000; in press).

5. Results

5.1. Strait of Gibraltar

At the Mediterranean side of the straits, the surface of zero velocity between the Atlantic and Mediterranean waters can be defined by the salinity of 37.8 (Garcia Lafuente et al., 2000). At station 6, Mediterranean waters almost reach the surface, while at the southern station 8, the Atlantic waters inflow extends

to the depth of almost 100 m (Fig. 2a). Large particulate matter (LPM) distribution shows high concentrations near the Spanish coast on the north-eastern part of the Gibraltar Strait. Mean LPM carbon weight per cubic meter in the superficial 100 m at the station 6 is $149 \mu\text{g C l}^{-1}$, one order of magnitude higher than the value obtained at the southern station 8, which is $21 \mu\text{g C l}^{-1}$ (Fig. 2b).

The LPM distribution in the superficial layer follows the isohalines. Turbidity peaks in the superficial 100 m with higher integrated concentrations on the northern side, decreasing southward. Turbidity and LPM concentrations are negatively correlated with the size of particles. At station 6 between 400 and 600 m, where the concentration of particles is low, their size is in the upper range. Below this depth, we observe a population of small particles (not shown). Data on integrated particle concentrations and carbon weight in the 0–100, 100–200, 200–800 and 800–1000 m layers for the characteristic stations are given in Table 1.

5.2. Almeria–Oran jet

Particles recorded by the UPV were divided into two size groups. The first containing particles between 200 and 500 μm diameter (Fig. 3b), the second with particles $>500 \mu\text{m}$ (Fig. 3c). The particles carbon mass and the fluorescence vertical pattern (Fig. 3a) from 0 to 250 m was plotted along a South–North transect.

Station 2 was positioned in an anticyclonic gyre, station 1 at the right side of the jet core, station 5 at the left side of the jet core, station 6 in the jet divergence, station 4 in the Mediterranean side of the divergence and station 3 in the adjacent Mediterranean waters. The highest concentration of the small particulate matter (200–500 μm) in the water column was found at the right side of the jet at station 1 (Fig. 3b and d) where the deepest vertical extent of the algal fluorescence (130 m, Fig. 3a) was measured. Station 2 located in the anticyclonic eddy showed low superficial concentrations but an increase in intermediate depths (200–400 m) and a deep peak at 700 m. A peak of large particles at the surface as well as in deeper layers was detected at station 5 (Fig. 3c). Station 6 was the site of the highest primary production. The largest particles were recorded at station 5 and progressively decreased in size north and south of

this location (Fig. 4). LPM standing stocks (0–100) in the jet were 4–10-folds higher than in the adjacent water masses (Table 1). At station 2, in the deep layers the concentration of particles increased, probably due to resuspension from the nearby Algerian continental slope.

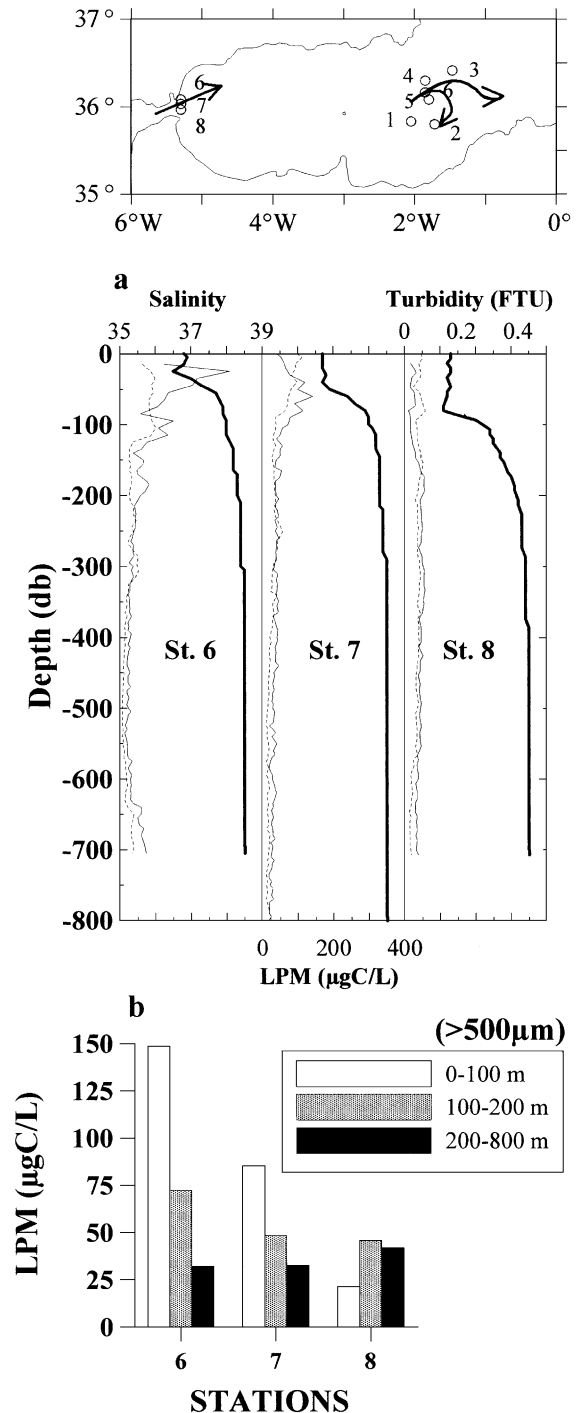
5.3. Algerian eddies

During the ELISA 1 cruise conducted in summer 1997, we focused sampling on an Algerian (anticyclonic) eddy (called 96-1), ~ 180 km in diameter and with a vertical extent down to the seafloor (~ 2800 m). A small cyclonic shear eddy generated at a coastline break by the large anticyclonic eddy was also sampled. Detailed descriptions of these eddies are given in Puillat et al. (2002) and Taupier-Letage et al. (in press).

High LPM concentration and turbidity maxima were located in the upper central layer of the cyclonic eddy (Fig. 5a) and corresponded to the fluorescence maximum (not shown), located between 40 and 80 m. The central station showed the highest LPM (Fig. 5c) and turbidity concentrations in the upper 100 m, in agreement with the phytoplankton distribution. Below 400 m the turbidity values decreased. Particles size distribution was inversely correlated to the concentration. In other words, size of particles increased with decreasing concentration.

The anticyclonic eddy 96-1 (Fig. 5b) displayed the characteristic structure with depressed isohalines in the central zone. Its eastern edge was located in the vicinity of the stations 117 and 119 (shallow isohalines), where fluorescence below 200 m (Taupier-Letage et al., in press) was detected. Turbidity values were high in the superficial layer and in the fluorescence maximum. Fluorescence and turbidity vertical extent showed a similar pattern, deepening from the eddy's edge subsurface downward along the isopycnals (Fig. 5b). LPM maxima were observed at 70 m at the station 119, at the depths of 100, 110 and 150 m,

Fig. 2. Large particulate matter (LPM) and turbidity vertical distribution in the Strait of Gibraltar. Only the north–south section of the Mediterranean transect is shown here. (a) Salinity (heavy line), LPM distribution expressed in carbon weight (continuous thin line) and turbidity (in Formazin Turbidity Units). (b) Mean LPM carbon per liter in three depth layers. Above: blow up of the studied zone. Arrows designate the superficial flow field.



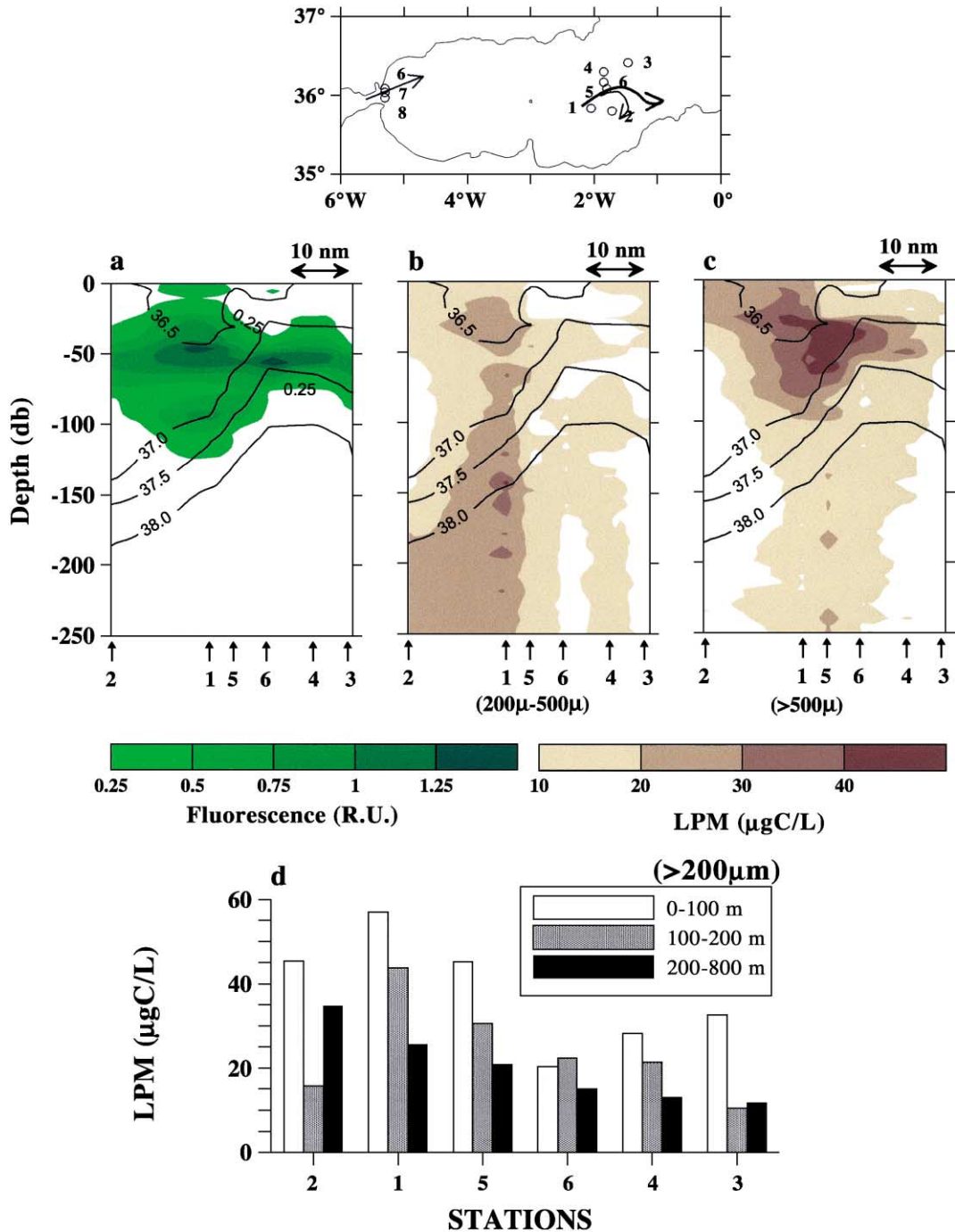


Fig. 3. Contour plots of the fluorescence and of the LPM spatial distribution in the cross-section of the Almeria–Oran jet. (a) Fluorescence, (b) 200–500 μm LPM size class and (c) >500 μm LPM size class, (d) mean LPM carbon per liter in the three depth layers. The stations are positioned by latitude.

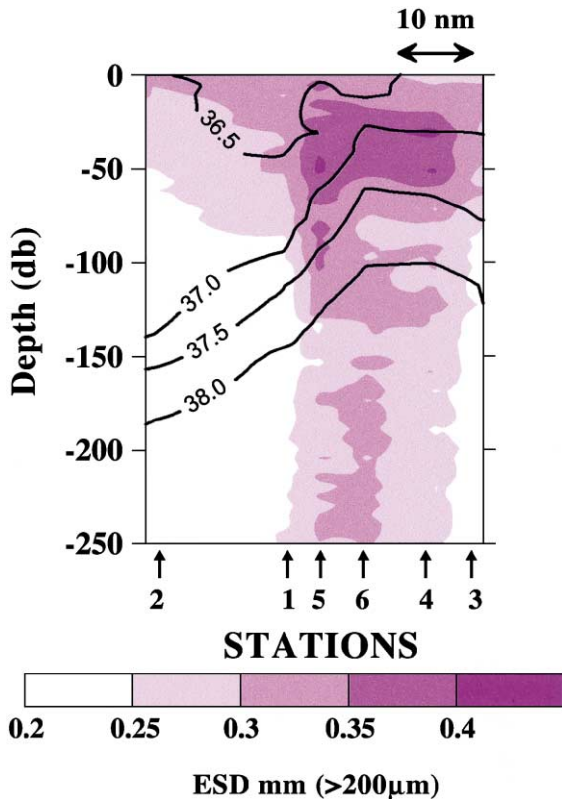


Fig. 4. LPM size distribution (in equivalent spherical diameters) in the cross-section of the Almeria–Oran jet.

respectively, at stations 117, 115 and 114, from the edge to the center of the eddy (Fig. 5d). At the station 114, the LPM spread vertically down to 250 m. Beneath this depth and down to 470 m, the LPM concentration decreased. The deep LPM concentrations were high at the eastern part of the transect and at the stations 105 and 103 near the center of the eddy. The eastern station (no. 121) was considered to be located on the outer side of the eddy.

5.4. The Northern Current

5.4.1. Liguro-Provençal Front

The section crossing the Northern Current between Nice and Calvi (Corsica) in the Ligurian Sea was intensively studied during the MBP Front program between 1992 and 1996 (Stemmann, 1998). Transects were performed every second month across the current, the adjacent frontal zone and also in the open sea

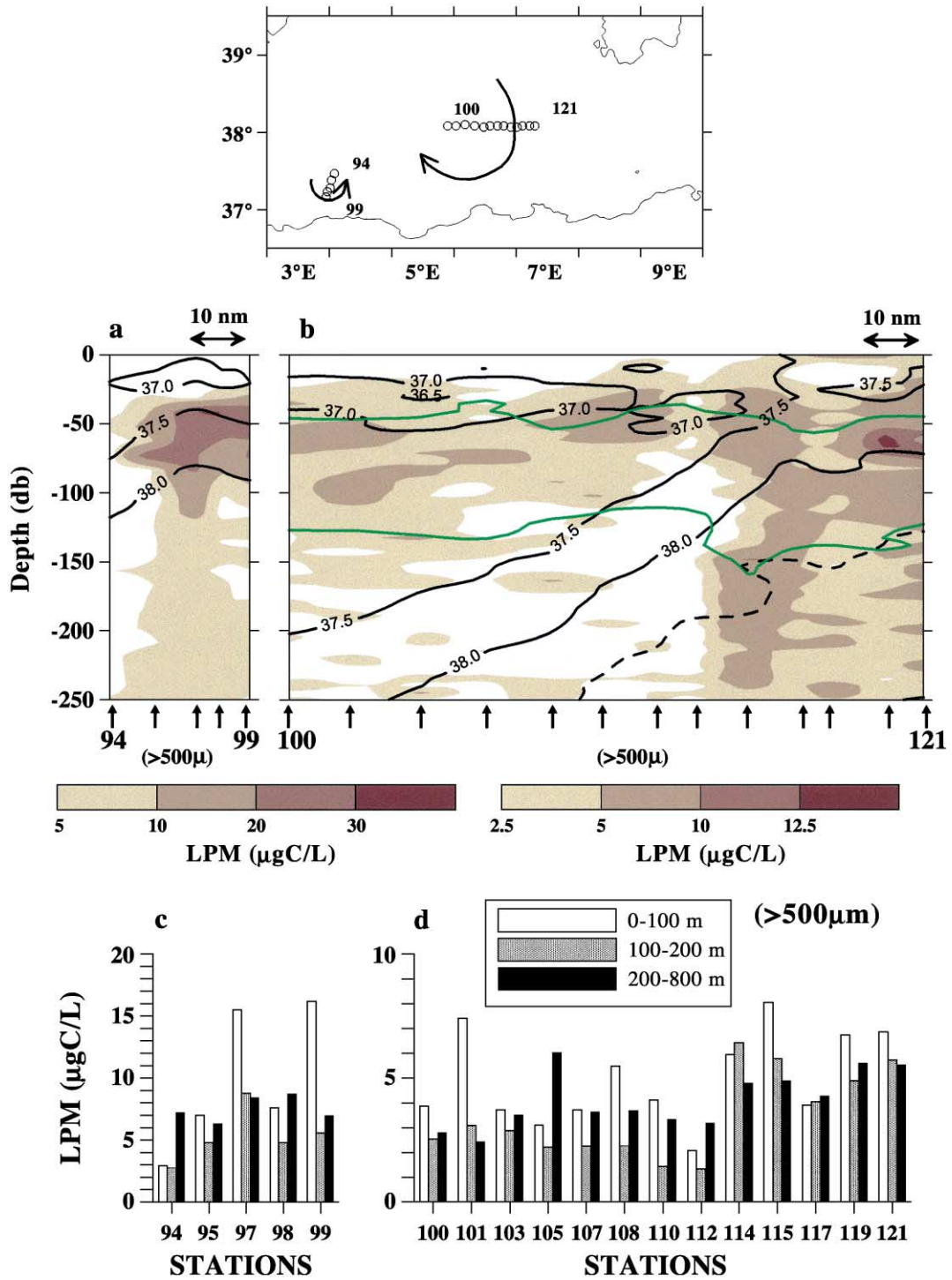
at the site of the long term station DYFAMED, 28 nautical miles (nm) offshore (Fig. 6). In July 1995, the section presented here, the current was about 14 nm large and relatively shallow. The main photosynthetic production was measured on the open sea side and one part of the produced biomass was apparently downwelled toward the coast (Fig. 6a). Large particulate matter (LPM) recorded by the Underwater Video Profiler (UVP) was divided into two size classes. The first included particles from 200 to 500 μm and the second particles $>500 \mu\text{m}$ equivalent spherical diameter.

LPM in both size classes was concentrated near the coast. The carbon mass was greater in the smaller LPM size class (Fig. 6a). Several particle rich nepheloid layers were observed near the slope. Larger particles displayed higher concentrations from 10 to 13 nm offshore, under the frontal zone (Fig. 6b). The LPM concentrations at the open sea stations including the DYFAMED station were very low, exhibiting a typical oligotrophic regime (Fig. 6c).

5.4.2. Gulf of Lions

The transect off Marseille in the eastern part of Gulf of Lions (Fig. 1) was studied in 1995, during the European EMPS MTP program. The circulation of the water masses and of the particulate matter in the Gulf of Lions is mostly driven by the cyclonic circulation of the Northern Current. The Rhone River input of particulate matter and the shelf processes have an enriching effect on the superficial LPM concentrations near the continental slope. The fluorescence and LPM maximums were observed near the shelf. Offshore, the LPM concentrations were low (Table 1). The subsuperficial and deep LPM concentrations off Marseille and at the DYFAMED site off Nice displayed similar values. Both stations were located about 50 km offshore.

The transect off Banyuls in the western part of the Gulf of Lions (Fig. 7) showed high fluorescence values in the superficial layers near the coast. The open sea upper layers were characterized by larger LPM size classes than at the coastal stations. The general pattern of the LPM distribution in the water column near the slope demonstrated that the PM on the upper slope formed a permanent intermediate nepheloid layer composed mainly of small particles (Fig. 7a, station B3). Below 400 m, the concentration of particles decreased and the proportion of large



particles increased. LPM concentrations at the near-shore station (B3, Table 1) were high. Mean carbon concentration between 100 and 200 m reached approximately $50 \mu\text{g C l}^{-1}$ (Fig. 7b). Offshore the values rapidly decreased reaching the mean open sea value of $3 \pm 1 \mu\text{g C l}^{-1}$.

The Banyuls transect was conducted during the European EUROMARGE program in 1995. During the same program, one transect was carried out north to Balearic Islands (Table 1, S3 and S5, Fig. 1), where higher values were observed near the coast and low values in the open sea.

5.5. The PROSOPE cruise

During this 35-day-long cruise conducted in August and September 1999, we sampled most of the regions studied during the programs described above. Most of the features studied before 1999 are persistent or permanent features. Therefore, the PROSOPE cruise served as a control for the long-term validity of the observed trends. LPM concentrations sampled during the PROSOPE cruise in the Western Mediterranean were within the limits observed in the specific studies. The highest values were in the superficial 100 m ($52 \mu\text{g C l}^{-1}$) near the Gibraltar Strait, $42 \mu\text{g C l}^{-1}$ in the vicinity of the Almeria–Oran jet and $25 \mu\text{g C l}^{-1}$ in the Algerian basin. The lowest were measured at the Ligurian open sea station. LPM concentrations in the Thyrrenian basin were similar to those found to the south of Sardinia (Fig. 8, station 4, Table 2).

6. Discussion

6.1. Mesoscale physical structures and LPM concentration

According to Rodriguez et al. (2001), the ubiquitous mesoscale structures such as eddies or jets generate frontal systems in which the ageostrophic vertical circulation directly controls the size structure of phytoplankton. The upward motion may compen-

sate for the sinking velocities of large phytoplankton and aggregates and may contribute to the explanation of their superficial patchiness. During one decade, we have studied different mesoscale features in the Mediterranean. We have observed that the LPM distribution in the water column is spatially heterogeneous. While Rodriguez et al. (2001) focused on the effect of upward motion on the size structure of large phytoplankton, we investigated the effect of possible downward motion on the distribution of LPM. Different processes mediate particles to the ocean's interior such as: sedimentation or mass sedimentation (Turley and Mackie, 1995), vertical mixing, aggregation and vertical migration of secondary producers, reaggregation of small particles by the midwater fauna and others. The downwelling generated by highly energetic mesoscale flow fields is one of the processes enabling the vertical flux of surface produced biogenic matter. In oligotrophic environments, fertilization due to mesoscale structures may play a key role in the local biological production and vertical fluxes. However, the Mediterranean is a small sea and the coastal influence should be taken into consideration when investigating mesoscale processes.

6.1.1. Atlantic inflow

Hydrodynamics in the Strait of Gibraltar is determined by the two-layer inverse estuarine circulation (Armi and Farmer, 1988). The semidiurnal tidal currents are an important source of variability. These oscillations generate expansion–contraction dynamics in the superficial 200 m, which is reflected in the variability of the LPM vertical distribution (Echevarria et al., in press). During the September 1997 CANIGO cruise, the highest chlorophyll *a* and LPM concentrations occurred at station 6 (near the Spanish coast, Fig. 2). At this location, the phytoplankton was composed of a high proportion of large algal cells, mainly diatoms. LPM concentrations decreased toward the south (the African coast) where the flow velocity is high. The Atlantic inflow extends nearly 100 m deep (Garcia Lafuente et al., 2000) and the interface is dissociated from the thermocline resulting in lower chlorophyll concentrations (Rodriguez et al., 1998).

Fig. 5. LPM ($>500 \mu\text{m}$) distribution contour plots in the (a) north–south transect through the cyclonic eddy (stations 94–99), (b) east–west half transect performed from the center to the eastern edge of the anticyclonic eddy 96-1 during the ELISA 1 cruise. Isohalines are plotted for both structures, the $0.25 \mu\text{g}$ chlorophyll *a* envelope is plotted only for the anticyclonic eddy; (c) and (d) as in Fig. 3. (Arrows = sampled stations).

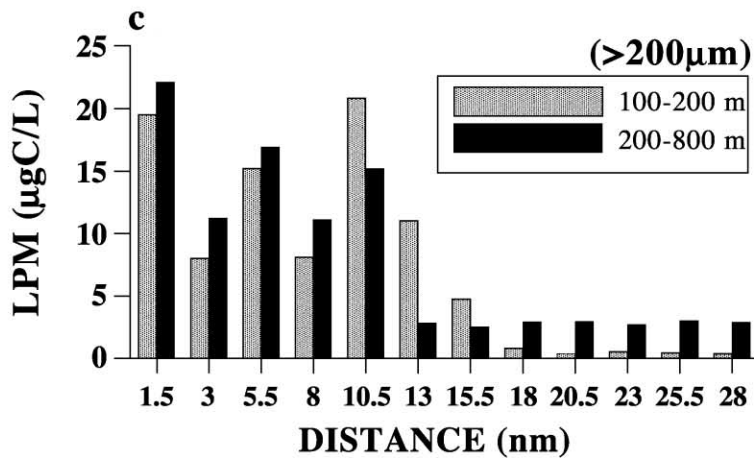
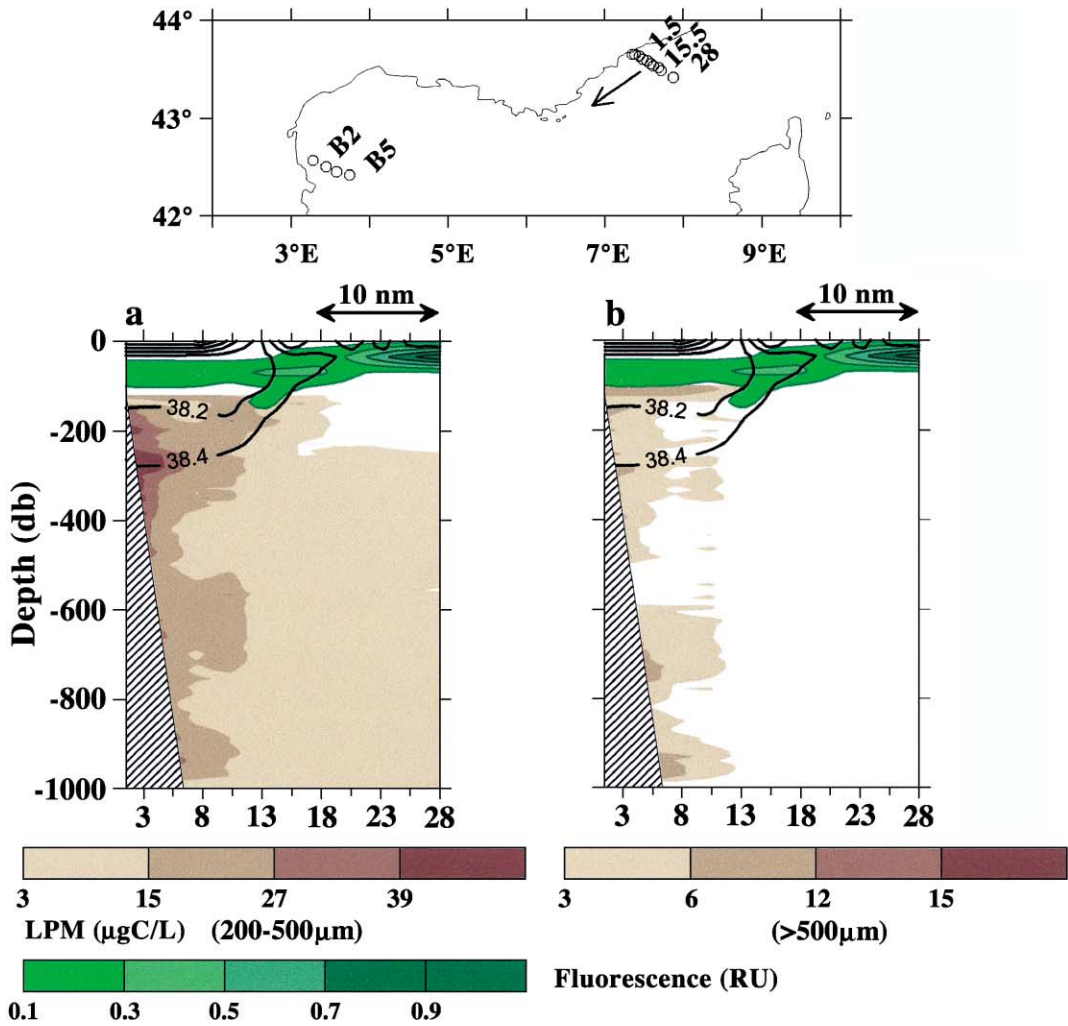


Table 1

Mean LPM concentration in number per liter and mean carbon weight measured during six different projects

| Initial depth | Latitude | Longitude | Mean LPM concentration ($\# \text{ l}^{-1}$) | | | | Mean carbon weight ($\mu\text{gC m}^{-3}$) | | | | Index of site |
|---------------|----------|-----------|--|---------|---------|----------|--|---------|---------|----------|---------------|
| | | | 0–100 | 100–200 | 200–800 | 800–1000 | 0–100 | 100–200 | 200–800 | 800–1000 | |
| 0 | 36.1 | 5.3 | 109.0 | 60.4 | 26.9 | | 148.6 | 73.8 | 32.5 | | 1 |
| 0 | 36.0 | 5.3 | 18.7 | 40.7 | 35.7 | | 21.4 | 45.7 | 42.2 | | 1 |
| 17 | 35.8 | 1.7 | 2.0 | 7.1 | 9.7 | 10.5 | 2.3 | 7.4 | 10.7 | 14.4 | 2 |
| 0 | 35.8 | 2.1 | 23.6 | 10.5 | 9.2 | 7.9 | 34.5 | 13.3 | 11.7 | 11.3 | 2 |
| 16 | 36.4 | 1.5 | 6.5 | 2.5 | 3.5 | 3.4 | 7.8 | 2.7 | 3.4 | 3.6 | 2 |
| 0 | 37.5 | –4.1 | 2.7 | 2.4 | 6.3 | 4.5 | 2.9 | 2.8 | 7.2 | 5.6 | 3 |
| 0 | 37.3 | –4.0 | 13.4 | 7.3 | 8.3 | 5.9 | 15.9 | 8.7 | 8.5 | 6.4 | 3 |
| 65 | 37.2 | –4.0 | 14.4 | 5.3 | 6.9 | 5.4 | 17.4 | 5.6 | 7.0 | 5.8 | 3 |
| 5 | 38.1 | –5.9 | 3.9 | 2.7 | 2.8 | 2.5 | 3.9 | 2.6 | 2.8 | 2.6 | 4 |
| 20 | 38.1 | –6.3 | 3.0 | 2.3 | 5.6 | 5.6 | 3.2 | 2.2 | 6.0 | 6.5 | 4 |
| 0 | 38.1 | –7.3 | 6.3 | 5.4 | 5.1 | 4.8 | 6.8 | 5.7 | 5.6 | 5.4 | 4 |
| 45 | 39.1 | –14.7 | 7.7 | 2.8 | 3.0 | 3.6 | 8.8 | 2.9 | 3.1 | 3.7 | 5 |
| 24 | 41.9 | –10.5 | 5.5 | 2.6 | 3.6 | 3.6 | 5.9 | 2.7 | 3.7 | 3.7 | 6 |
| 100 | 43.6 | –7.4 | | 4.8 | 3.9 | 6.8 | | 5.1 | 3.8 | 6.7 | 7 |
| 100 | 43.4 | –7.9 | | 0.2 | 0.5 | 0.8 | | 0.2 | 0.6 | 0.9 | 7 |
| 10 | 43.0 | –5.2 | 14.8 | 33.7 | 10.0 | 4.6 | 17.0 | 38.4 | 11.3 | 4.5 | 10 |
| 10 | 42.8 | –5.2 | 8.5 | 2.6 | 2.2 | 3.2 | 9.5 | 2.7 | 2.2 | 3.3 | 10 |
| 50 | 42.5 | –3.5 | 16.8 | 20.4 | 39.4 | | 21.3 | 22.7 | 49.7 | | 11 |
| 40 | 42.4 | –3.8 | 8.7 | 3.2 | 5.3 | 4.2 | 12.2 | 3.9 | 5.7 | 5.1 | 11 |
| 50 | 41.8 | –4.3 | 8.0 | 2.4 | 1.9 | 2.3 | 11.7 | 3.1 | 2.2 | 2.9 | 12 |
| 10 | 40.1 | –3.6 | 6.2 | 6.4 | 10.8 | | 7.9 | 7.3 | 11.5 | | 12 |
| 10 | 40.2 | –3.5 | 0.3 | 0.4 | 2.2 | 3.8 | 4.5 | 3.3 | 2.2 | 4.0 | 12 |

Initial depth corresponds to the depths where data treatment started. Data reported here corresponds to the labels shown in Fig. 9. 1-CANIGO, 2-ALMOFRONT, 3-ELISA cyclonic shear eddy, 4-ELISA anticyclonic eddy, 7-MBP-Front and 10, 11 and 12-EUROMARGE sections off Marseille, Banyuls and Balearic Islands. The Thyrrenian profiles (8, 9 on Fig. 8) were indexed here as 5 and 6. The exhaustive data set can be obtained upon request.

Table 2

Comparison between the carbon weight ($\mu\text{g C l}^{-1}$) of the PROSOPE cruise (1999) and the former cruises in the western Mediterranean

| PROSOPE cruise mean carbon weight | | | | | | Other cruises mean carbon weight | | | | | |
|-----------------------------------|---------------|-------|---------|---------|----------|----------------------------------|---------------|-------|---------|---------|----------|
| Station label | Initial depth | 0–100 | 100–200 | 200–800 | 800–1000 | Station label | Initial depth | 0–100 | 100–200 | 200–800 | 800–1000 |
| Station 1 | 25 | 52.3 | 11.1 | 16.4 | 16.4 | CANIGO2 Station 6 | 0 | 148.6 | 73.8 | 32.5 | |
| Station 2 | 30 | 42.8 | 10.9 | 6.6 | 6.6 | ALMOFRONT1 | 0 | 34.5 | 13.3 | 11.7 | 14.4 |
| | | | | | | Station 1 | | | | | |
| Station 3 | 35 | 24.7 | 4.3 | 2.9 | 2.9 | ELISA Station 99 | 65 | 17.4 | 5.6 | 7.0 | 5.8 |
| Station 4 | 45 | 7.2 | 2.9 | 2.8 | 2.8 | ELISA Station 100 | 5 | 3.9 | 2.7 | 2.8 | 2.5 |
| Station 8 | 45 | 7.4 | 3.1 | 3.0 | 3.0 | | | | | | |
| Station 9 | 24 | 7.3 | 3.1 | 3.7 | 3.7 | | | | | | |
| Station DYF | 0 | 1.5 | 0.9 | 1.7 | 1.7 | MBP Front Station 28 | 100 | | 0.2 | 0.6 | 0.9 |

Stations 4, 8 and 9 (Fig. 8) were not sampled by the UVP before 1999.

Phytoplankton accumulates near the zero velocity layer where the advection is low. The interface between the two water masses was shallow in the

northern part of the Strait, where the nutrient rich water could appear in the euphotic layer and contribute to the increase of LPM concentrations. The complex but

Fig. 6. Small (200–500 μm) (a) and larger, >500 μm LPM distribution (b), during the MBP Front transect between the coast and the open Ligurian Sea (distances from the coast in nautical miles—nm) in July 1995. The isohalines and the fluorescence (in green) were measured from the surface, the LPM from 100 to 1000 m depth. The continental slope is on the left side of the plot; the DYFAMED site on the right side; (c) as in Fig. 3.

regular mixing processes within the sill region periodically fertilize the surface waters. This pulsing enrichment together with the shallow interface may explain the high standing stock of chlorophyll and LPM on the northern, Mediterranean side of the Strait. The Atlantic inflow forms an anticyclonic gyre (the western Alboran gyre) stimulating high biological activity observed during the CANIGO and PROSOPE programs near Spain (Figs. 2 and 8; Tables 1 and 2). Calculated mean LPM carbon values in September 1997 near the Spanish coast were extremely high ($149 \mu\text{g C l}^{-1}$ in the superficial layer). They decreased with depth but remained high when compared to other Western Mediterranean sites (Table 1).

The Gibraltar Strait station sampled during the PROSOPE cruise was located 9 km east of the station studied during the CANIGO program in 1997. This difference in location as well as the spatial heterogeneity of the LPM engendered by high energy hydrological processes (Rodríguez and Li, 1994) and the variability of the coastal influence may be the reasons for the lower LPM concentrations found in 1999 ($52 \mu\text{g C l}^{-1}$). Nevertheless, the values we obtained at the north-eastern part of the Gibraltar Straits during the PROSOPE cruise were within the limits of LPM variability observed during the CANIGO cruises and are among the highest in the Western Mediterranean.

6.1.2. Almeria–Oran jet

During the US Coastal Transition Zone Program (CTZ), Dewey et al. (1991) examined the frontal dynamics along an offshore flowing filament. They found submesoscale divergences and convergences resulting in upwelling and downwelling of water masses along isopycnal surfaces. According to Washburn et al. (1991) superficial water masses can be downwelled by vertical circulation related to a strong offshore jet. They remove large quantities of organic matter from the euphotic to the aphotic layers. During the CTZ program Kadko et al. (1991) measured vertical subduction velocity of 27 m day^{-1} based on ^{222}Rn sampling of the filaments off Northern California. They proposed that the deep chlorophyll maxima are derived from subducted surface layers and not from in situ production.

In the Mediterranean, the geostrophic flow of the Almeria–Oran jet, studied during the ALMOFRONT

program, was the site of higher biological productivity than the adjacent oligotrophic systems (Fig. 3). The results were published in 1994 in the special issue on Processes and Fluxes in the Geostrophic Almeria–Oran Front in *Journal of Marine Systems* (vol. 5, 187–399).

The ageostrophic circulation associated with the main flow was characterized by enhanced biological activity. The upwelled nutrients boosted the primary production and one part of the resulting biomass could be downwelled along the isopycnal surfaces (Videau et al., 1994; Zakardjian and Prieur, 1998) until it could undergo cross-isopycnal sedimentation. Larger particles sedimented out through the isopycnals first, the small particles were transported farther away from the site of their production (Fig. 4). Within the Alboran Sea, the Atlantic inflow generates two anticyclonic gyres, but only the western gyre is quasi-permanent. The presence and activity of the eastern gyre determines the position of the geostrophic jet. When the eastern gyre is active, the jet flows from the vicinity of Almeria, Spain toward Oran, Algeria. When the activity of the gyre is low, the jet is found in a southern position, along the 1000 m isobath. This was its position during the ALMOFRONT1 cruise. The left side of the jet is characterized by strong frontal dynamics (Prieur and Sournia, 1994). Gould and Wiesenburg (1990) found in the vicinity of this frontal zone concentrations of chlorophyll reaching $23 \mu\text{g l}^{-1}$, produced by a monospecific algal population, the diatom *Thalassiosira partheneia*. Send et al. (1999) have also observed a strong horizontal density gradient in the Alboran Sea generated by the interaction of Atlantic and Mediterranean waters. Fluorescence and ADCP backscatter data clearly indicated downward motions along the isopycnals. Similar features were observed by Tintoré et al. (1986) and confirmed by Tintoré et al. (1998). Both water masses, Atlantic and Mediterranean, are considered as oligotrophic and thus frontal fertilization may play a key role in the local biological production.

In 1991, surface velocities of about 90 cm s^{-1} were measured in the Almeria–Oran jet core. Phytoplankton biomass was significantly higher in the jet area than elsewhere. The Almeria–Oran geostrophic front generated a secondary circulation characterized by isopycnal downwelling. The velocity of this transport was estimated as 10 cm s^{-1} . According to Videau

et al. (1994), one part of the enhanced phytoplankton production at station 6 was downwelled along the inclined isopycnals to the depth of 80 m at station 5 and 110 m at the station 1. The intense algal production increased the zooplankton biomass and its feeding activity (Thibault et al., 1994). The secondary production was sustained by the locally enhanced production within time scales allowing the development of grazers with a relatively long generation time.

Among the stations presented in Fig. 3, the stations situated in the jet displayed the highest values. The northern station 3 was a typically oligotrophic Mediterranean station, while the southern station was poor in LPM at the subsurface but relatively rich in the deep layers. This enrichment was probably due to the resuspension from the nearby continental slope.

In a 300-m deep trap at the southern station, Peinert and Miquel (1994) found that the particulate matter had a high POC:chl *a*-equiv. ratio, typical for aged detritus. They also found that diatom frustules and other remains were devoid of organic matter. Particulate silica flux was also high at 300 m, as well as the mass flux. Conversely, the mass fluxes determined by sediment traps were low at 100 m. These results were consistent with the observations made by the UVP (Fig. 3), i.e., low LPM concentrations occurred in the superficial 150 m and increased with depth. Our conclusion, that small particles may be carried southward by isopycnal transport from the superficial frontal stations to deeper layers, agreed with the conclusions of Peinert and Miquel (1994).

6.1.3. Eddies

The incoming Atlantic water generally flows eastward along the Algerian slope and is called the Algerian Current. According to Millot (1985) and Obaton et al. (2000), this current is baroclinically unstable and forms meanders enclosing anticyclonic eddies that propagate eastward. Shallow transient cyclonic circulations can also form at the meander crest, as well as small cyclonic shear eddies, generated at coastline breaks, but they are superficial and also short-lived.

As observed in Fig. 5, the shear cyclonic eddy concentrated high quantities of LPM in the superficial central layer. A transient structure such as this small shear eddy may thus substantially increase the bio-

logical production in oligotrophic waters. This is not the case with the anticyclonic eddies. McGillicuddy et al. (1998) suggested that the shoaling density surfaces can induce an upward flux of nutrients fixed by the phytoplankton, whereas deepening density surfaces push nutrient-depleted water out of the surface layers.

In the eddy 96-1, chlorophyll *a* and LPM vertical extent increased from the edge to the center and was detected below 150 m (Fig. 5). Below 470 m, two vertical structures can be observed with a higher standing stock of LPM carbon (Fig. 10), one below the outer part of the edge (station 121) and the second near the center of the eddy. Station 121 is considered to be located on the outer side of the eddy. Mass fluxes observed here in sediment traps (ELISA data, in preparation) were the highest at the eastern station. This result may indicate that the fluxes and the LPM stock observed at the far East of 96-1 during the ELISA 1 cruise resulted from local production. For example, the 3 μ M nitrate isopleth was noticed above the 38 isohaline. This may suggest that the Mediterranean water contributes to the local production (Taupier-Letage, personal observation).

Higher LPM concentrations located below 470 m at stations 105 and 103 were situated in the prolongation of the higher turbidity (small particles, blue contour plot; Fig. 10) values. Unfortunately, the discrete sampling performed was not fine enough to provide a detailed coverage of the processes at edges (tow-yo data were recorded earlier with a SeaSoar in 96-1. Southampton Oceanographic Center, data processing ongoing). However, we noted (1) a deepening from the edge to the center of the fluorescence and LPM maximum layer, (2) an increase in turbidity ensuing the subduction of phytoplankton and (3) a size shift in the particles toward larger sizes dominating the water column below the central part of the anticyclonic eddy. The spatial distribution of fine and coarse particles from nephelometer and LPM data, respectively, (Fig. 10) may suggest an isopycnal transport followed by a cross-isopycnal sedimentation and aggregation but obviously, more data is needed to support this hypothesis.

6.2. Coastal processes

Continental margins are strongly influenced by seasonally intense upwelling, river inputs or slope

currents. Such periodic input of nutrients is likely to produce high spatial and seasonal variability in biological activity and consequently in LPM production. Topography of the margins plays an important role in channeling the particulate matter down the slope. Canyons are particularly important off-shelf transport pathways (Gardner, 1989; Monaco et al., 1990). Particle fluxes reaching deep layers are closely linked to upper layer bio-physical processes. However, they not only reflect the balance between the euphotic zone production and loss rates, but are influenced by general processes such as remineralisation (Turley and Stutt, 2000), scavenging aggregation or lateral advection (Asper et al., 1992; Neuer et al., 1997).

6.2.1. The Northern Current

Nepheloid layers associated with the continental slope were observed in all the cruises conducted during the 39-month MBP-Front survey in the Ligurian Sea (Stemmann, 1998). Seasonal variability in the size spectrum was more pronounced than the variability of LPM abundances. In winter and spring, the mean LPM size was greater than during the other seasons. The sub-superficial nepheloid layer was related to the horizontal density gradient (Gorsky et al., 2000). Near the coast, the midwater nepheloid layer was often positively correlated with the deep scattering layer (DSL), determined by a 38-kHz echosounder (Baussant et al., 1993). Terrestrial input, slope erosion by the Northern Current or the subduction of the superficial biological production are the most frequently mentioned origins of the aphotic LPM. Only occasionally did the nepheloid layers extend to the open sea. Long distance offshore transport of particles was observed mostly as result of winter storms followed by heavy river discharge. In summer, the sub-superficial and deep LPM concentrations off Nice decreased from the coast seaward (6-fold in the 200–800 m layer). Concentrations in the open sea, DYFAMED station (DYF in Fig. 8, 28 nm offshore), were the lowest in the western basin (Figs. 6 and 8; Tables 1 and 2). The Northern Current and the deeper LIW that follow isobaths in the same westward, along-slope direction (Millot, 1990; Durrieu de Madron et al., 1990) are advecting the particulate matter along the coast but are also maintaining this matter near shore, reducing its seaward dilution. This biomass enriched by the matter subducted by the

frontal activity has important implications for benthic and midwater fauna feeding and recruitment success (Gorsky et al., 1991; Pedrotti, 1993).

6.2.2. Gulf of Lions and Balearic Sea

The continental margin of the Gulf of Lions is characterized by a complex seafloor topography including several canyon systems. In Gulf of Lions, part of the particulate matter is transferred from the entrance of the system (transect off Marseille, Table 1) to the western exit at the Pyrenean margin (the western transect off Banyuls, Fig. 7, Table 1). Particulate matter from the Rhône river and the resuspended slope material are advected westward. Although LPM concentrations in the superficial 200 m are higher in the Gulf of Lions entrance (off Marseille) than at the exit side, below 200 m off Banyuls, the LPM density is very high ($\sim 50 \mu\text{g C l}^{-1}$). The nearby canyon discharge, along slope advection, deep resuspension, as well as local primary production are all likely to contribute to the high LPM concentrations observed on the shelf break during the EURO-MARGE cruise (Fig. 7, Table 1).

Heussner et al. (1993) defined two types of margins (1) oceanic: characterized by a decreasing flux and (2) continental: where the flux increases with depth. Although the LPM concentration from 150 to 300 m was high near the Banyuls continental slope (station B3, Fig. 7), the offshore export was low. The LPM either rapidly reached the slope sediments or was transported westward. On the northern Spain margin, Puig et al. (2000) found that suspended particle fluxes were 360 times higher on the open slope than the settling particle fluxes. This indicates that the advective along slope transport dominates over the settling particle fluxes. Below 100 m at the open sea station SC (off Banyuls), LPM concentrations were low and corresponded to the typical open sea LPM concentrations found in the Western basin (Table 1, Fig. 9).

During the EUROMARGE cruise, a transect was performed from the Balearic islands northward. The results show a rapid decrease of the LPM concentrations from the coast toward the open sea (5-fold in the 200–800 m layer; Fig. 9, Table 1). Although the superficial values were lower than in Gulf of Lions, the rapid decrease of the LPM concentrations from the coast toward the open sea is in agreement with the results obtained in the Ligurian Sea and Gulf of Lions.

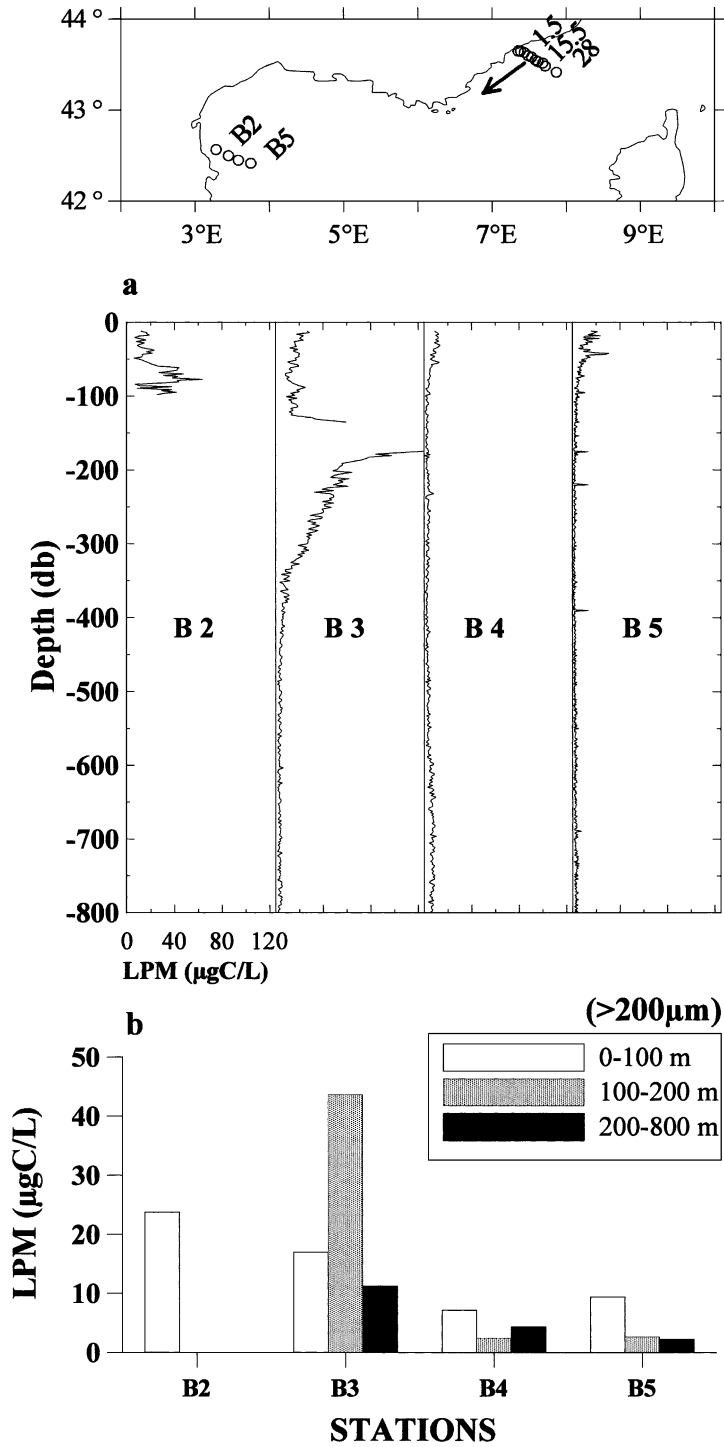


Fig. 7. LPM (>200 μm) vertical distribution off Banyuls (western part of the Gulf of Lions) expressed in carbon weight (a). The LPM concentration on the shelf break, profile B3, exceeded the threshold limits set up for natural particles and could not be treated; (b) as in Fig. 3.

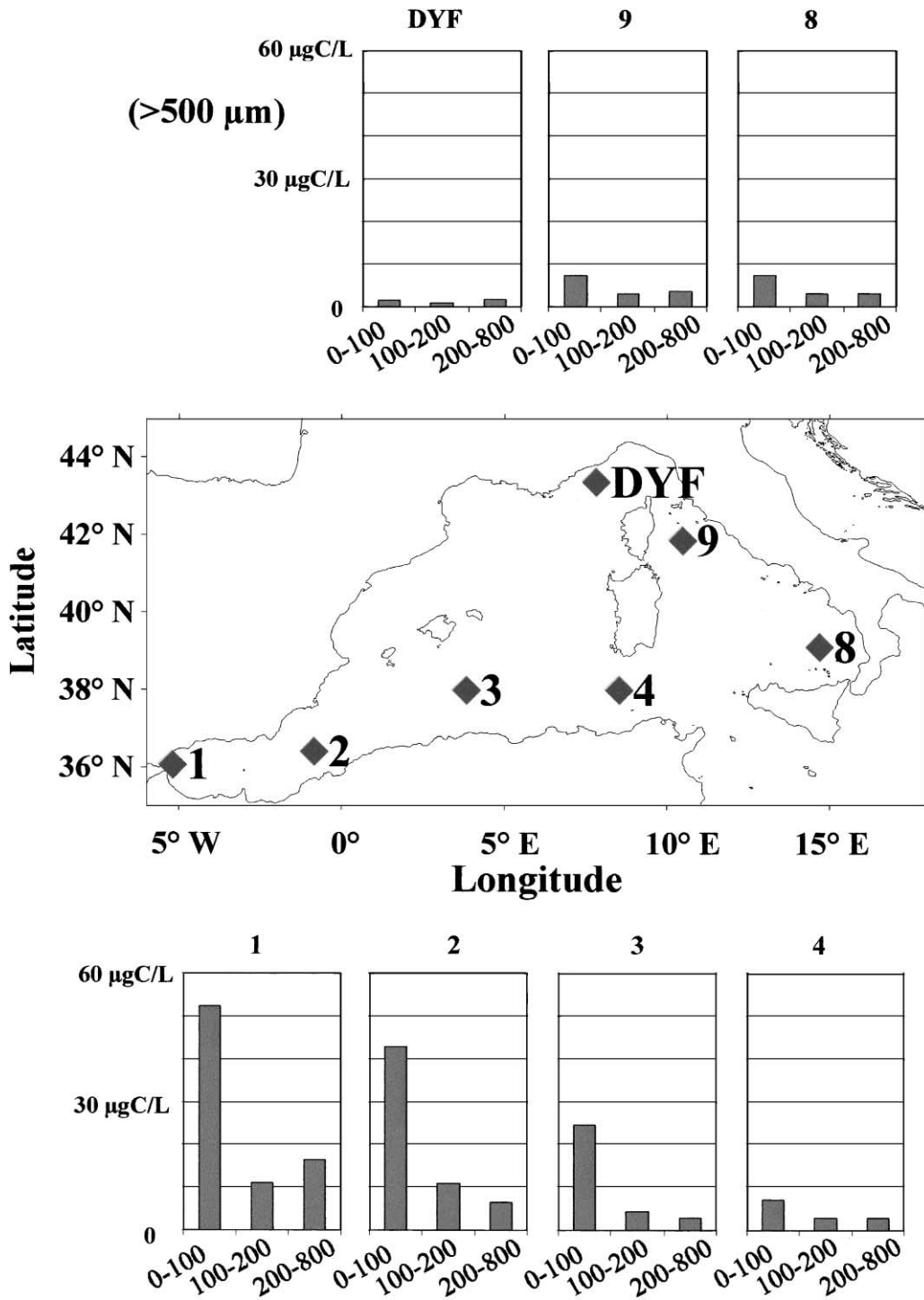


Fig. 8. PROSOPE cruise western Mediterranean sampling sites (diamonds) and the calculated mean LPM carbon weight in three depth layers for LPM $>500 \mu\text{m}$.

7. The PROSOPE cruise

In September 1999, during the PROSOPE cruise the Alboran Sea, Algerian basin, Thyrrhenian Sea and Ligurian Sea were revisited (Fig. 8, Table 2). This cruise provided a good opportunity to validate the observations made during the different programs carried out since 1991 in the Western Mediterranean. At a first glance, the diminishing LPM concentrations from the Strait of Gibraltar toward the Ligurian Sea could suggest a relationship with the progressive mixing of Atlantic waters. However, the different mesoscale studies reported above show a variability in the LPM concentrations with high values related to the mesoscale structures (10–100 km). We consider as mesoscale features the frontal structures associated to jets, currents, eddies and also the structures associated to the continental slope studied during the EUROMARGE program.

In order to test the hypothesis suggested by the PROSOPE results, we plotted the values of all the characteristic stations (Table 1), assigning an index to each mesoscale program (site, Fig. 9). Indices 1–7 are organized in order of increasing distance from the Strait of Gibraltar. The distance between the two sites is approximately 500 km. Stations in each site were

generally within a 50-km distance. For comparison, we plotted in Fig. 9 the PROSOPE stations and connected the different depth layers. The EUROMARGE sites, indices 10, 11 and 12 are separated because of the low Atlantic influence and the coastal influence.

The site index 1 (Strait of Gibraltar) shows the highest LPM concentrations while the central Ligurian Sea (index 7) shows three orders of magnitude lower. High concentrations can be observed near the Gulf of Lions shelf (indices 10 and 11). Except at the Strait of Gibraltar, the low values observed at the other sites are similar: between 2 and 4 $\mu\text{g C l}^{-1}$. Stations exhibiting low values are at a distance inferior to 50 km from stations having high LPM content. This variability may be attributed to the influence of mesoscale dynamic structures such as fronts of currents separating stations with low and high biological production. As a consequence, mesoscale features may create high LPM concentrations close to impoverished water masses. It is important to note that the low LPM values are similar in all the Western Mediterranean basin, independently of the distance from Gibraltar. Some of the stations with high LPM content are influenced by the coastal processes (CANIGO station 6, ELISA station 99,

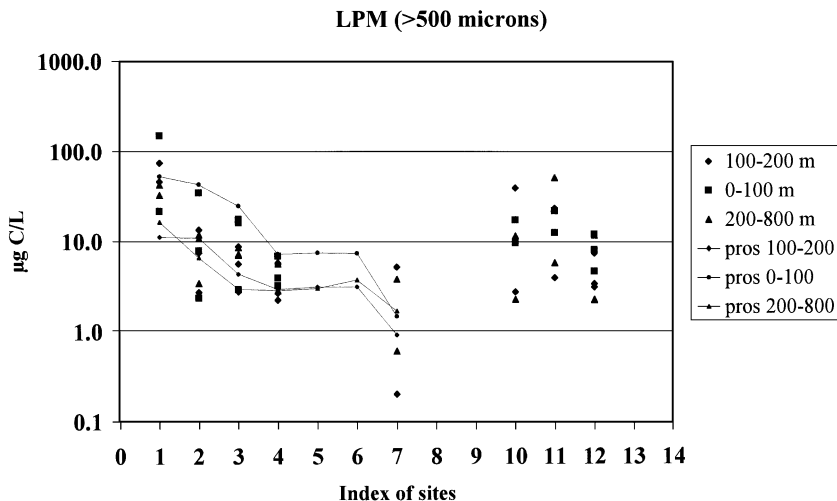


Fig. 9. Mean LPM carbon concentration in three different layers for different stations (see Tables 1 and 2). The x-axis index number is related to the increasing distance of different sampled sites from the Gibraltar Strait. In increasing order: 1 — CANIGO, 2 — ALMOFRONT, 3 — ELISA cyclonic shear eddy, 4 — ELISA anticyclonic eddy, 7 — MBP-Front and 10, 11 and 12 — EUROMARGE sections off Marseille, Banyuls and Balearic Islands. The index corresponding to the location of the sampled site was given to the PROSOPE stations (1, 2, 3, 4, 8, 9 and DYF, empty symbols). The Thyrrhenian profiles (8, 9 on Fig. 8) were indexed here as 5 and 6. pros = PROSOPE stations.

MBP-Front station 5.5) others are associated to open sea fronts (ALMOFRONT station 1, ELISA stations 97 and 121). We observe an eastward decline in the upper range of the LPM concentrations. This can be the consequence of the increasing oligotrophy. However, the mesoscale structures enhance locally the biological production as shown by the one order of magnitude high variation of LPM concentration in each site.

In conclusion, the LPM spatial distribution is directly related to the mesoscale physical structures and to the continental slope. The highest LPM values decrease with the distance from Gibraltar, but the low values remain similar in the whole western basin. Therefore, the eastward decrease of LPM concentrations observed during the PROSOPE cruise is fortuitous and depends on the distance of the sampled stations from the productive zones.

However, the LPM concentrations found during the PROSOPE cruise are within the limits of variability observed in corresponding sites during the past programs.

8. Conclusions

In the superficial 200 m of the oligotrophic Ligurian Sea, the calculated LPM carbon constitutes 4–34% of filtered carbon (GF/F filters, 0.7 μm porosity). Thus, up to one third of the pool of particulate matter might be composed of large particles (Stemmann et al., 2000). On the other hand, the fraction of particulate organic carbon (POC) exported daily from the euphotic layer to 1000 m depth is about 10% in the Gulf of Lions, rapidly decreasing seaward (Danovaro et al., 1999). An important part of the POC and PON

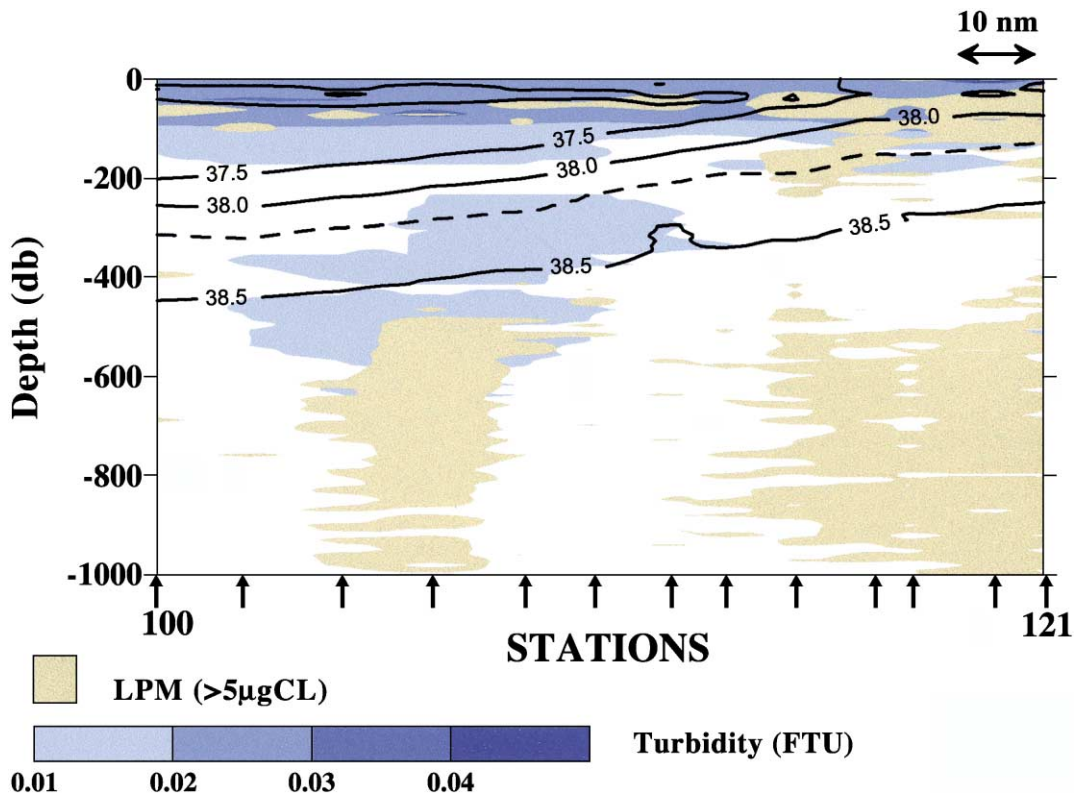


Fig. 10. Turbidity (blue contour plot, nephelometer data) and LPM (concentrations $>5 \mu\text{g C l}^{-1}$) spatial structure in the anticyclonic eddy 96-1 studied during the ELISA program. The isohalines are superimposed. Note the deepening of the turbidity and the LPM from the edge of the eddy toward its center and the overlapping position of the LPM and the turbidity in the deep layers under the anticyclonic eddy center. The stations number is given in Fig. 5d.

is sequestered in the water column in the form of large particles. The results from the Ligurian Sea suggest that the LPM standing stock in the first kilometer equals 2–3 months of vertical flux (Stemmann, 1998). However, the LPM content in the water column can change within shorter time scales (Graham et al., 2000; Stemmann et al., 2000). Shifts in the trophic regime, in the bacterial activity or in the zooplankton population dynamics can rapidly modify the fate of the particulate matter.

Surface hydrodynamics stimulate the biological production and the export of particulate matter. Physical structures such as jets, gyres, eddies or geostrophic currents induce vertical motions allowing nutrient injection and/or large phytoplankton accumulation in superficial layers, and thus the formation of LPM. The convective downwelling may transport the water and its content along the isopycnals. The size of the particulate matter influences its vertical export. According to our observations, large particles sediment out first and small particles are being advected on longer distances and may participate in the process of LPM formation in deeper layers (Fig. 10). Therefore, the physically induced downward export of the superficial production can be “size fractionated” and contributes to the heterogeneous particulate spatial distribution of the LPM.

From the comparison of the results obtained during 1999 PROSOPE cruise with the results from former studies, we can deduce the following:

1. results acquired during the last decade are consistent with those from 1999;
2. the mesoscale physical structures may enhance the biological production by about one order of magnitude and induce a spatially heterogeneous distribution of LPM;
3. the highest LPM values are found in the Strait of Gibraltar and the lowest in the open Ligurian Sea;
4. in the western basin's main, below 100 m, the lower LPM concentration range is remarkably homogenous varying between 2 and 4 $\mu\text{g C l}^{-1}$;
5. the cross-slope transport suggests that the sedimentation rates are high near the slope and that the export rates to the open sea are low.

Acknowledgements

We acknowledge the support from the European Commission's Marine Science and Technology Program (MAST II and III) under contracts MAS2-CT94-0090 (EMPS project), MAS3-CT96-0060 (CANIGO project), MAS3-CT96-0051 (MATER project) and MAS3-CT98-0161 (EURAPP project). The INSU/CNRS (JGOFS/France) and the University Paris 6 co-funded this study. We thank Marsh Youngbluth and Beat Gasser for helpful discussions, J.M. Grisoni for the microprocessor design, J.C. Lemonnier for the technical help, the chief scientists and the crews of different research vessels for the field assistance.

References

- Allredge, A.L., 1979. The chemical composition of macroscopic aggregates in two neritic seas. *Limnol. Oceanogr.* 24, 855–866.
- Allredge, A.L., 1998. The carbon, nitrogen and mass content of marine snow as function of aggregate size. *Deep-Sea Res., Part I* 45, 529–541.
- Allredge, A.L., Gotschalk, C.C., 1988. In situ settling behavior of marine snow. *Limnol. Oceanogr.* 33, 339–351.
- Allredge, A.L., McGuillivray, P., 1991. The attachment probabilities of marine snow and their implications for particle coagulation in the ocean. *Deep-Sea. Res.* 38, 431–443.
- Allredge, A.L., Silver, M.W., 1988. Characteristics, dynamics and significance of marine snow. *Progr. Oceanogr.* 20, 41–82.
- Armi, L., Farmer, D.M., 1988. The flow of Mediterranean water through the Strait of Gibraltar. *Progr. Oceanogr.* 21, 1–105.
- Arnone, R.A., La Violette, P.E., 1986. Satellite definition of the bio-optical thermal variation of coastal eddies associated with the African current. *J. Geophys. Res.* 91, 2351–2364.
- Arnone, R.A., Wisemburg, D.A., Saunders, K.D., 1990. The origin and characteristics of the Algerian current. *J. Geophys. Res.* 95, 1587–1598.
- Asper, V.L., Honjo, S., Orsi, T.H., 1992. Distribution and transport of marine snow in Panama Basin. *Deep-Sea Res.* 39, 939–952.
- Baussant, T., Gasser, B., Gorsky, G., Kantidakis, A., 1993. Mesopelagic micronekton and macrozooplankton observed by echosounding, multiple—net sampling and video profiling across the Almeria–Oran front (W. Mediterranean Sea). *Ann. Inst. Oceanogr.* 69, 87–95.
- Bethoux, J.P., Morin, P., Chaumery, C., Connan, O., Gentili, B., Ruiz-Pino, D., 1998. Nutrients in the Mediterranean Sea, mass balance and statistical analysis of concentrations with respect to environmental change. *Mar. Chem.* 63, 155–169.
- Bethoux, J.P., Gentili, B., Morin, P., Nicolas, E., Pierre, C., Ruiz-Pino, D., 1999. The Mediterranean Sea: a miniature ocean for climatic and environmental studies and a key for the climatic functioning of the North Atlantic. *Progr. Oceanogr.* 44, 131–146.

- Boucher, J., Ibanez, F., Prieur, L., 1987. Daily and seasonal variations in the spatial distribution of zooplankton populations in relation to the physical structure in the Ligurian front. *J. Mar. Res.* 45, 133–173.
- Chester, R., Stoner, H., 1974. The distribution of particulate organic carbon and nitrogen in some surface waters of the world ocean. *Mar. Chem.* 2, 263–275.
- Copin-Montegut, C., 1993. Alkalinity and carbon budgets in the Mediterranean Sea. *Global Biogeochem. Cycles* 7, 915–925.
- Danovaro, R., Dinet, A., Duineveld, G., Tselepides, A., 1999. Benthic response to particulate fluxes in different trophic environments: a comparison between the Gulf of Lions–Catalan Sea (western-Mediterranean) and the Cretan Sea (eastern-Mediterranean). *Progr. Oceanogr.* 44, 287–312.
- Dewey, K.R., Moum, J.N., Clayton, A.P., Caldwell, D.R., Pierce, S.D., 1991. Structure and dynamics of a coastal filament. *J. Geophys. Res.* 96, 14886–14908.
- Durrieu de Madron, X., Nyffeler, F., Godet, C.H., 1990. Hydrographic structure and nepheloid spatial distribution in the Gulf of Lions continental margin. *Cont. Shelf Res.* 10, 915–929.
- Echevarria, F., et al. Physical–biological coupling in the Strait of Gibraltar. *Deep-Sea Res.*, in press.
- Franks, P.J.S., Walstad, L.J., 1997. Phytoplankton patches at fronts: a model of formation and response to wind events. *J. Mar. Res.* 55, 1–29.
- Garcia Lafuente, J., Vargas, J.M., Plaza, F., Sarhan, T., Candela, J., Bascheck, B., 2000. The tide at the eastern section of the Strait of Gibraltar. *J. Geophys. Res.* 105, 14197–14214.
- Gardner, W.D., 1989. Baltimore Canyon as a modern conduit of sediment to the deep sea. *Deep-Sea Res.* 36, 323–358.
- Gardner, W.D., Walsh, I.D., 1990. Distribution of macroaggregates and fine-grained particles across a continental margin and their potential role in fluxes. *Deep-Sea Res.* 37, 401–411.
- Gomez, F., et al., 2000. Microplankton distribution in the Strait of Gibraltar: coupling between organisms and hydrodynamic structures. *J. Plankton Res.* 22 (4), 603–617.
- Gorsky, G., Lins Da Silva, N., Dallot, S., Laval, P., Braconnot, J.C., Prieur, L., 1991. Midwater Tunicates: are they related to the permanent front of the Ligurian Sea (northwestern Mediterranean)? *Mar. Ecol. Progr. Ser.* 74, 195–204.
- Gorsky, G., Aldorf, C., Kage, M., Picheral, M., Garcia, Y., Favole, J., 1992. Vertical distribution of suspended aggregates determined by a new underwater video profiler. *Ann. Inst. Oceanogr.* 68, 275–280.
- Gorsky, G., Picheral, M., Stemmann, L., 2000. Use of the Underwater Video Profiler for the study of aggregate dynamics in the North Mediterranean. *Estuarine, Coastal Shelf Sci.* 50, 121–128.
- Gould Jr., R.W., Wiesenburg, D.A., 1990. Single species dominance in a subsurface phytoplankton concentration at a Mediterranean Sea front. *Limnol. Oceanogr.* 35, 211–220.
- Graham, W.M., MacIntyre, S., Alldredge, A.L., 2000. Diel variations of marine snow concentration in surface waters and implications for particle flux in the sea. *Deep-Sea Res., Part I* 47, 367–396.
- Guerzoni, S., et al., 1999. The role of atmospheric deposition in the biogeochemistry of the Mediterranean Sea. *Progr. Oceanogr.* 44, 147–190.
- Guilén, J., Palanques, A., Durrieu de Madron, X., Nyffeler, F., 2000. Field calibration of optical sensors for measuring suspended sediment concentration in the Western Mediterranean. *Sci. Mar.* 64, 427–435.
- Hall, I.R., Schmidt, S., McCave, I.N., Reyss, J.L., 2000. Particulate matter distribution and $^{(234)}\text{Th}/^{(238)}\text{U}$ disequilibrium along the northern Iberian margin: implications for particulate organic carbon export. *Deep-Sea Res. Part I* 47, 557–582.
- Herut, B., Krom, M., 1996. Atmospheric input of nutrient and dust to the SE Mediterranean. In: Guerzoni, S., Chester, R. (Eds.), *The Impact of Desert Dust Across the Mediterranean*. Kluwer Academic Publishers, Dordrecht, pp. 349–358.
- Heussner, S., Monaco, A., Carbone, J., 1993. Biogenic particle transfer on the NW Mediterranean continental margin: a summary of ECOMARGE results. *Ann. Inst. Oceanogr.* 69, 141–145.
- Honjo, S., Doherty, K.W., Yogesh, C., Agrawal, Y.C., Asper, V.L., 1984. Direct optical assessment of large amorphous aggregates (marine snow) in the deep ocean. *Deep-Sea Res.* 31, 67–76.
- Jackson, G.A., Logan, B.E., Alldredge, A.L., Dam, H.G., 1995. Combining particle size spectra from a mesocosm experiment using photographic and aperture impedance (Coulter and Elzone) techniques. *Deep-Sea Res., Part II* 42, 139–157.
- Jackson, G.A., Maffione, R.E., Costello, D.K., Alldredge, A.L., Logan, B.E., Dam, H.G., 1997. Particle size spectra between 1 μm and 1 cm at Monterey Bay determined using multiple instruments. *Deep-Sea Res.* 44, 1739–1768.
- Kadko, D.C., Washburn, L., Jones, B., 1991. Evidence of subduction within cold filaments of the northern California coastal transition zone. *J. Geophys. Res.* 96, 14909–14926.
- Lampitt, R.S., Hilier, W.R., Challenor, P.G., 1993. Seasonal and diel variation in the open ocean concentration of marine snow aggregates. *Nature* 362, 737–739.
- Lohrenz, S.E., Arnone, R.A., Wisenburger, D.A., De Palma, L.P., 1988. Satellite detection of transient enhanced primary production in the Western Mediterranean Sea. *Nature* 335, 245–247.
- MacIntyre, S., Alldredge, A.L., Gotschalk, C.C., 1995. Accumulation of marine snow at density discontinuities in the water column. *Limnol. Oceanogr.* 40, 449–468.
- McGill, D.A., 1970. Mediterranean sea atlas. The distribution of nutrient chemical properties. *Woods Hole Oceanogr. Inst. Atlas Ser.* 3, 97–110.
- McGillicuddy, D.J., Robinson, A.R., Siegel, D.A., Jannasch, H.W., Johnson, R., Dickey, T.D., McNeil, J., Michaels, A.F., Knap, A.H., 1998. Influence of mesoscale eddies on new production in the Sargasso Sea. *Nature* 394, 263–266.
- Millot, C., 1985. Some features of the Algerian current. *J. Geophys. Res.* 90, 7169–7176.
- Millot, C., 1990. The Gulf of Lion's hydrodynamics. *Cont. Shelf Res.* 10, 885–894.
- Millot, C., 1999. Circulation in the Western Mediterranean Sea. *J. Mar. Syst.* 20, 423–442.
- Millot, C., Benzohra, M., Taupier-Letage, I., 1997. Circulation off Algeria inferred from the Mediprod-5 current meters. *Deep-Sea Res.* 44, 1467–1495.
- Monaco, A., Biscaye, P.E., Soyer, J., Pocklington, R., Heussner, S., 1990. Particle fluxes and ecosystem response on a continental

- margin during the 1985–1988 Mediterranean ECOMARGE experiment. *Cont. Shelf Res.* 10, 809–839.
- Moutin, T., Raimbault, P., 2002. Primary production, carbon export and nutrients availability in western and eastern Mediterranean Sea in early summer 1996 (MINOS cruise). *J. Mar. Syst.*, 33–34, 273–288 (this issue).
- Neuer, S., Ratmayer, V., Davenport, R., Fischer, G., Wefer, G., 1997. Deep water particle flux in the Canary Island region: seasonal trends in relation to long-term satellite derived pigment data and lateral sources. *Deep-Sea Res., Part I* 44, 1451–1466.
- Obaton, D., Millot, C., Chabert d’Hières, G., Taupier-Letage, I., 2000. The Algerian Current: comparisons between in situ and laboratory measurements. *Deep-Sea Res.* 47, 2159–2190.
- Pedrotti, M.L., 1993. Spatial and temporal patterns of distribution of echinoderm larvae in the Ligurian Sea (Mediterranean sea): implications on recruitment. *J. Mar. Biol. Assoc. U. K.* 73, 513–530.
- Peinert, R., Miquel, J.C., 1994. The significance of frontal processes for vertical particle fluxes. A case study in the Alboran Sea (SW Mediterranean Sea). *J. Mar. Syst.* 5, 377–390.
- Prieur, L., Sournia, A., 1994. Almofront-1 (April–May 1991): an interdisciplinary study of Almeria–Oran geostrophic front, SW Mediterranean Sea. *J. Mar. Syst.* 5, 187–204.
- Puig, P., Palanques, A., Guillén, J., Garcia-Ladona, E., 2000. Deep slope currents and suspended particle fluxes in and around the Foix submarine canyon (NW Mediterranean). *Deep-Sea Res., Part I* 47, 343–366.
- Puillat, I., Taupier-Letage, I., Millot, C., 2002. Algerian Eddies lifetime can near 3 years. *J. Mar. Syst.* 31, 245–259.
- Rodriguez, J., Li, W.K.W., 1994. The size structure and metabolism of the pelagic ecosystem. *Sci. Mar.* 58, 1–167.
- Rodriguez, J., Blanco, J.M., Jimenez-Gomez, F., Echevarria, F., Gil, V., Rodriguez, V., Ruiz, J., Bautista, B., Guerrero, F., 1998. Patterns in the size structure of the phytoplankton community in the deep fluorescence maximum of the Alboran Sea (south-western Mediterranean). *Deep-Sea Res.* 454, 1577–1593.
- Rodriguez, J., Tintoré, J., Allen, J.T., Blanco, J.M., Gomis, D., Reul, V., Rodriguez, V., Echevarria, F., Jimenez-Gomez, F., 2001. Mesoscale vertical motion and the size structure of phytoplankton in the ocean. *Nature* 410, 360–363.
- Send, U., Font, J., Krahnmann, G., Millot, C., Rhein, M., Tintoré, J., 1999. Recent advances in observing the physical oceanography of the Western Mediterranean Sea: a review. *Progr. Oceanogr.* 44, 37–64.
- Sournia, A., Brylinsky, J.M., Dallot, S., Le Corre, P., Leveau, M., Prieur, L., Froget, C., 1990. Fronts hydrologiques au large des côtes françaises. Les sites ateliers du programme “Frontal”. *Oceanol. Acta* 13, 413–428.
- Southerland, T.F., Lane, P.M., Amos, C.L., Downing, J., 2000. The calibration of optical backscatter sensors for suspended sediment of varying darkness levels. *Mar. Geol.* 162, 587–597.
- Spall, S.A., Richards, K.J., 2000. Numerical model of mesoscale frontal instabilities and plankton dynamics: I. Model formulation and initial experiments. *Deep-Sea Res., Part I* 47, 1261–1301.
- Stemmann, L., 1998. Particulate matter spatio-temporal analysis using a new video system, in the north-western Mediterranean Sea. Influence of biological production, terrestrial inputs and hydro-dynamical forcing. Doctorat de l’Université Paris VI, 180 pp.
- Stemmann, L., Picheral, M., Gorsky, G., 2000. Diel variation in the vertical distribution of particulate matter (>0.15 mm) in the NW Mediterranean Sea investigated with the Underwater Video Profiler. *Deep-Sea Res., Part I* 47, 507–534.
- Stemmann, L., Gorsky, G., Marty, J.C., Picheral, M., Miquel, J.C., in press. Four years survey of large particles (>0.15 mm) vertical distribution (0–1000 m) in the NW Mediterranean. *Deep-Sea Res.*
- Suzuki, N., Kato, K., 1953. Studies on suspended materials. Marine snow in the sea: Part I. Source of marine snow. *Bull. Fac. Fish., Hokkaido Univ.* 4, 132–135.
- Syvitski, J.P.M., Asprey, K.W., Leblanc, K.W.G., 1995. In-situ characteristics of particles settling within a deep-water layer estuary. *Deep-Sea Res.* 42, 223–256.
- Taupier-Letage, I., Puillat, I., Raimbault, P., Millot, C. (in press). Biological response to mesoscale eddies in the Algerian Basin. *J. Geophys. Res.*
- Thibault, D., Gaudy, R., Le Fèvre, J., 1994. Zooplankton biomass, feeding and metabolism in a geostrophic frontal area (Almeria–Oran Front, Western Mediterranean). Significance to pelagic food webs. *J. Mar. Syst.* 5, 297–312.
- Tintoré, J., La Violette, P., Blade, P.E., Cruzado, A., 1986. A study of an intense density front in the eastern Alboran Sea: the Almeria–Oran front. *J. Phys. Oceanogr.* 18, 1384–1397.
- Tintoré, J., Gomis, D., Alonso, S., Parilla, G., 1991. Mesoscale dynamics and vertical motion in the Alboran Sea. *J. Physical Oceanogr.* 21, 811–823.
- Tintoré, J., Allen, J., Font, J., Corsini, G., Rodriguez, J., Gascard, J.C.OMEGA collaborators, 1998. Observation and modelling of eddy scale geostrophic and ageostrophic circulation. European Marine Science and Technology Conference. CEC. Edt. ISBN92-828-2898-0, 5–22.
- Turley, C.M., Mackie, P.J., 1995. Bacterial and cyanobacterial flux to the deep NE Atlantic on sedimenting particles. *Deep-Sea Res., Part I* 42, 1453–1474.
- Turley, C.M., Stutt, E.D., 2000. Depth-related cell-specific bacterial leucine incorporation rates on particles and its biogeochemical significance in the Northwest Mediterranean. *Limnol. Oceanogr.* 45, 419–425.
- Videau, C., Sournia, A., Prieur, L., Fiala, M., 1994. Phytoplankton and primary production characteristics at selected sites in the geostrophic Almeria–Oran front system (SW Mediterranean Sea). *J. Mar. Syst.* 5, 235–250.
- Viudez, A., Tintoré, J., Haney, R.L., 1996. Circulation in the Alboran Sea as determined by quasi-synoptic hydrographic observations: I. Three dimensional structure of the two anticyclonic gyres. *J. Phys. Oceanogr.* 26, 684–705.
- Washburn, L., et al., 1991. Water mass subduction and the transport of phytoplankton in coastal upwelling system. *J. Geophys. Res.* 96, 14927–14946.
- Zakardjian, B., Prieur, L., 1998. Biological and chemical signs of upward motions in permanent geostrophic fronts of the Western Mediterranean. *J. Geophys. Res.* 103, 27849–27866.